The Growth and Collapse of a Bubble between Parallel Flat Free Surfaces

[1]Toshiyuki Ogasawara*; [1]Seisuke Ito; [1]Hiroyuki Takahira

[1]*Osaka Prefecture University, 1-1 Gakuen-cho, Naka-ku, Sakai-shi, Osaka, JAPAN*

Abstract

The growth and collapse of a bubble between two parallel flat free surfaces and the corresponding water column formation on the free surfaces have been investigated experimentally and numerically. In the experiment, a laser-induced bubble generated inside a plane water jet and the dynamical motion of free surfaces were observed with a high-speed video camera. The results are characterized by two dimensionless parameters: the ratio of the maximum bubble radius to the water jet width, R_{max}^*, and the ratio of the initial bubble offset from the center line of the jet to the water jet width, ε^*. When a bubble is generated at the center ($\varepsilon^* = 0$), water columns are formed on both free surfaces during the growth phase of a bubble, following the formation of crown-like shaped water columns during the second growth and collapse of a bubble. Since the bubble does not translates, it grows and collapses at the center of the jet. However, a water column due to the bubble growth when $\varepsilon^* \neq 0$ tends to be formed only on the nearer free surface to the bubble during its growth phase. Then in the collapse phase the bubble translates toward the other free surface far from the bubble accompanying with a liquid-jet formation toward it. The liquid-jet and the rebound shockwave from the bubble cause the water column formation on both sides of free surfaces. Numerical simulations are conducted for the growth and collapse phases using the boundary element method (BEM) and for the collapse phase using the ghost fluid method (GFM). The water column formation during the growth phase, a toroidal bubble deformation during the collapse phase, and the translation of the collapsing bubble are well simulated by BEM. The result of GFM shows shockwave emission from the rebounding motion of the bubble which causes the water column formation when the shockwave impacts on the free surface with large curvature.

Keywords: bubble collapse; free surfaces; laser-induced bubble; boundary element method; ghost fluid method

Introduction

As a next generation nuclear spallation neutron source, liquid mercury jets are proposed as a novel target for various high-power nuclear and high-energy physics applications [1]. The cavitation bubbles within the jet which occur due to high-intensity pressure wave caused by the shock heating of the liquid-jet, however, raise target fragmentations and disturb a stable output of secondary particles. To predict the performance of those jets, the knowledge of the cavitation bubble behavior near free surfaces and/or inside those jets is necessary. The experiments and numerical analyses for the behavior of the bubble generated beneath a flat free surface were conducted by Chahine [2] and Blake and Gibson [3]. They showed that the bubble translates toward the direction away from the free surface during the bubble collapse phase. In addition, Chahine [2] found a limiting value above which the interaction between a bubble and a free surface is negligible. Afterwards, Robinson and Blake [4] and Tomita and Kodama [5] investigated the dynamics of single- and two-cavitation bubbles generated by a laser beam beneath a free surface. They concluded that the motion of two bubbles depends on the bubble size ratio and the distance between a bubble and a free surface. Zhang et al. [6] conducted the experiment for the behavior of the bubble generated beneath a free surface. They identified six distinctive patterns of free surface deformation accompanying the growth and collapse of the bubble. They also discussed the period of bubble oscillations, jet tip velocities, etc. Robert et al. [7] studied the growth and collapse of a laser-induced bubble inside an axisymmetric columnar water jet. They found that the shape and the timing of the ejection from columnar jet depend on the initial bubble position and the ratio of the bubble size to the jet diameter.

In the present study, we investigate the bubble collapse between two parallel free surfaces experimentally and numerically, and the influences of a bubble initial position and a maximum bubble size on its collapsing behavior and water column formations on the free surfaces are analyzed. In the experiment, a laser-induced bubble generated inside of a plain jet is observed using a high-speed video camera. The growth and collapse phases are simulated by

*Corresponding Author, Toshiyuki Ogasawara: oga@me.osakafu-u.ac.jp

the boundary element method (BEM) [8, 9] and the collapse phase is also simulated by the ghost fluid method [10-12].

Experimental study

Figure 1 shows schematic diagrams of an experimental setup and a nozzle geometry to form a plane jet, respectively. A nozzle outlet has a rectangular cross-section whose size is 3.4 mm x 26.0 mm and flat glasses are put on both ends in spanwise direction for the optical observation. To form a two-dimensional water jet in the streamwise direction, the shaded area on the glasses in Fig. 1(b) is coated so as to be hydrophobic. Nd: YAG laser (wavelength: 1064 nm, pulse energy: 325.0 mJ, beam diameter: 8 mm, pulse duration: 5-8 ns) is used to generate a laser-induced bubble in the plane water jet. The laser beam is collimated and focused by the achromatic lens whose focal length is 75 mm. Flow rate is 4.0 l/min and its corresponding average jet velocity is 0.75 m/s. Time scale of the bubble collapse is about 100 μs and it is so short that the effects of flow on the bubble behavior and the water column formation of the free surfaces are negligible. The bubble is generated about 8 mm below the nozzle and observed with a high-speed video camera. The frame rate and the exposure time are set to be 200 kfps and 0.4 μs, respectively. The shadow image of the bubble is visualized by the back illumination with a strobe light. The bubble size is controlled by an iris diaphragm and an initial bubble position is controlled by moving the nozzle in the perpendicular direction to the free surfaces using a linear stage. We introduce dimensionless time t^* which is a ratio of time t to the characteristic time of bubble collapse $t_0 = R_{max}(p_0/\rho)^{-0.5}$, here p_0 and ρ are the atmosphere pressure and the water density, respectively, and $t = 0$ s corresponds to the time of the laser emission. The results are characterized by two dimensionless parameters: the ratio of a maximum bubble radius to a water jet width, $R_{max}^* = R_{max}/w$, and the ratio of an initial bubble offset from the center line of the jet to a water jet width, $\varepsilon^* = \varepsilon/w$.

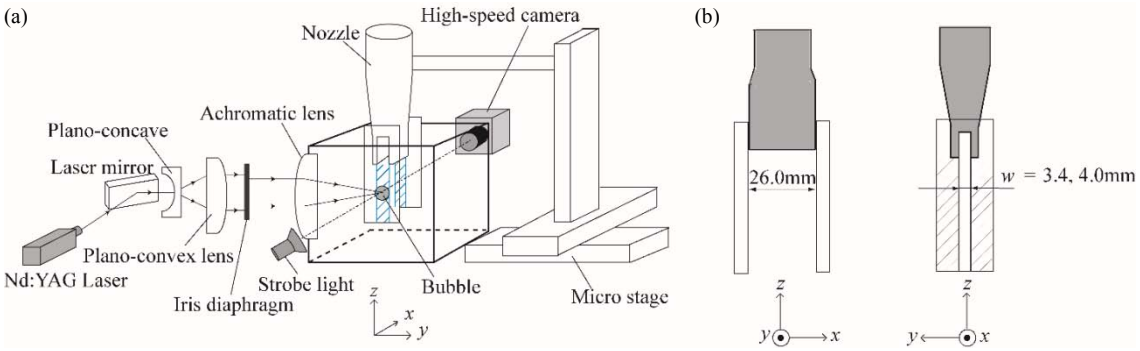

Figure 1 (a) Experimental setup and (b) the nozzle geometry.

The successive behaviors of a bubble and free surfaces are shown in Fig. 2 when the bubble is generated at the center of a plane water jet ($\varepsilon^* = 0$). Figures 2(i) and (ii) correspond to the cases of $R_{max}^* = 0.46$ and 0.61, respectively. The bubbles take the maximum volumes at the fourth top images (d). Initially, the bubble grows with horizontally long ellipsoidal shape. The bubble in Fig. 2(i) gradually becomes spherical shape during the growth phase. However, the bubble in Fig. 2(ii) keeps the horizontally long ellipsoidal shape at its maximum expansion. After the bubble volume becomes maximum, the bubble begins to shrink from the both sides near the free surfaces and collapses with vertically long ellipsoidal shape. In these cases with $\varepsilon^* = 0$, since the bubble position is symmetry to the plane water jet, the bubble centroid does not translate during the growth and collapse phases. The water columns are formed on both free surfaces. From the beginning of the bubble growth, the free surfaces gradually deform to be convex shape as the bubble grows. These deformations developing after the maximum expansion lead to water column formation normal to the free surfaces. Another type of water column formation is observed after the first rebound of the bubble. Crown-like shaped water columns surrounding the former water columns normal to the free surfaces develop afterwards. Both former and latter water columns grow more significantly when $R_{max}^* = 0.61$: the larger bubble case (Fig. 2(ii)).

Figure 3 shows the results in the case of $R_{max}^* \sim 0.5$ when the bubble initially offsets from the center line of the plane jet ($\varepsilon^* = 0.10, 0.18$). The bubble takes the maximum volume in (c). In the case of $\varepsilon^* = 0.10$, the collapsing behavior of the bubble and the free surface deformation are similar to those in the symmetric case in Fig. 2(i). The difference between these is that the bubble translates toward the farther (left) free surface slightly during the collapse

phase because of a slightly stronger effect of the nearer (right) free surface. In the case of $\varepsilon^* = 0.18$, however, a water column due to the bubble growth is formed only on the right free surface and grows with splash form. During the collapse phase, the bubble surface starts shrinking from a right side near the free surface, following a liquid-jet formation and penetration toward the left free surface. As a result, the bubble shape becomes toroidal and collapses at the center of the plane water jet. The liquid-jet and the rebound shockwave from the bubble cause the water column formation on the left free surface after the bubble collapses and rebounds.

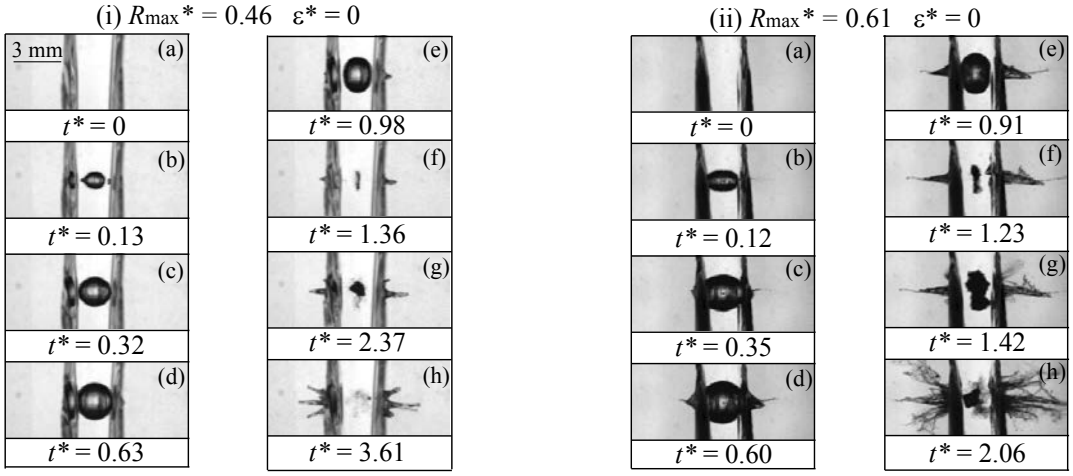

Figure 2 Snapshots of growth and collapse of a laser-induced bubble between free surfaces for $\varepsilon^* = 0$.

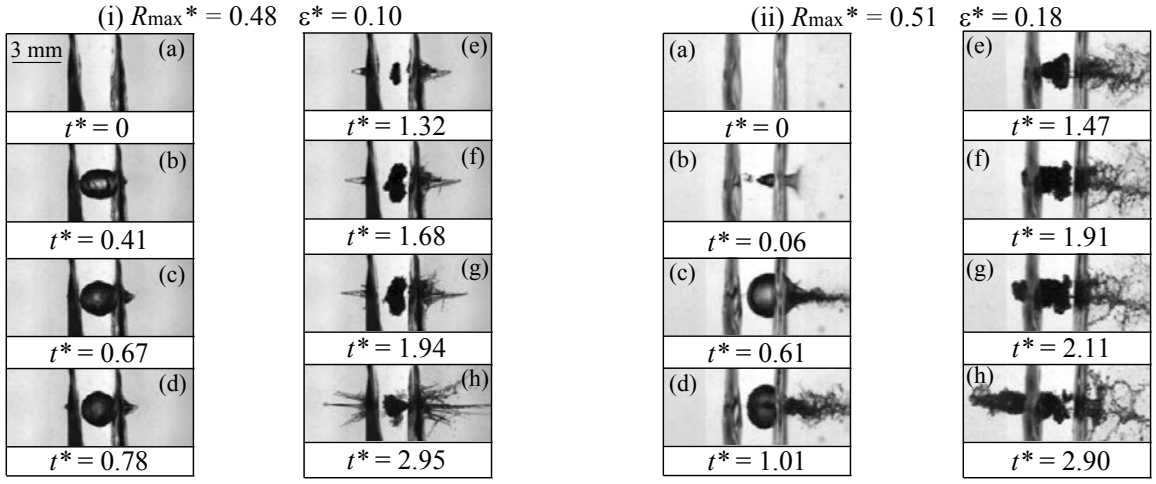

Figure 3 Snapshots of growth and collapse of a laser-induced bubble between free surfaces for asymmetric arrangement ($R_{max}^* \sim 0.5$).

Numerical studies

The above experiments are simulated using the boundary element method and the ghost fluid method. In the simulations, the axisymmetric situation in which the symmetry axis from the bubble center directs normally to the free surface is assumed.

The present boundary element analysis deals with the topological change in bubble shape using the method proposed by Best [13] and can simulate the toroidal bubble after a liquid-jet penetration. The initial ambient pressure in the liquid surrounding the bubble p_∞ is 10^5 Pa and the liquid density ρ_0 is 998.2 kg/m^3. The initial gas pressure inside the bubble p_{g0} is calculated from the integral form of Rayleigh-Plesset equation so that R_{max}^* takes the value of 0.47 (R_{max} = 1.88 mm). The mesh is divided non-uniformly into 405 on each free surface so as to arrange the finer meshes near the bubble, and the minimum size is $0.025R_{max}$. On the bubble surface, the boundary is divided into 32 meshes and the initial mesh size is $0.0048R_{max}$. The characteristic time is defined as $t_0 = R_{max}/(p_\infty/\rho)^{-0.5}$. Figure 4

shows the numerical results for symmetrical arrangement ((a) $\varepsilon^* = 0$) and asymmetrical one when the bubble initially offsets from the center line between the free surfaces ((b) $\varepsilon^* = 0.25$). The bubble grows and takes the maximum volume at the time in Fig. 4(a) (iii) to become a horizontally long ellipsoidal shape. After that, the bubble shrink begins from the both sides near the free surface. Development of the bubble surface instability leads to a biconcave disc shape during the collapse. Finally, the bubble is penetrated at the center of the disc shape and becomes toroidal shape. This toroidal bubble collapses accompanying with the liquid-jet formation from the inside of the torus to outside of the torus in Fig. 4(a) (vi-viii). On the other hand, the free surface begins to deform as the bubble grows and the water columns develop toward each outward normal direction. This development continues in the collapse phase which is consistent with the experimental result. For the asymmetrical arrangement (Fig. 4(b) $\varepsilon^* = 0.25$), the bubble grows with the translation towards the nearer (right) free surface, and the water column is formed only on this nearer (right) free surface. After the bubble takes the maximum volume in Fig. 4(b) (iii), the liquid-jet towards the farther (left) free surface develops and impact on the bubble surface. The toroidal bubble takes the minimum volume at the moment in Fig. 4(b) (vii), and rebounds afterwards as the bubble translates towards the liquid-jet direction (Fig. 4(b) (vii-x)). Under this condition, we could successfully simulate after the rebounding motion until another impact of the toroidal bubble surface occurs in Fig. 4(b) (x). In this case, not only the water column which develops during the growth and collapse phases on the right free surface, but also the other water column due to the liquid-jet penetration and the translation of the collapsing bubble on the left free surface is formed, which agrees qualitatively with the experimental results.

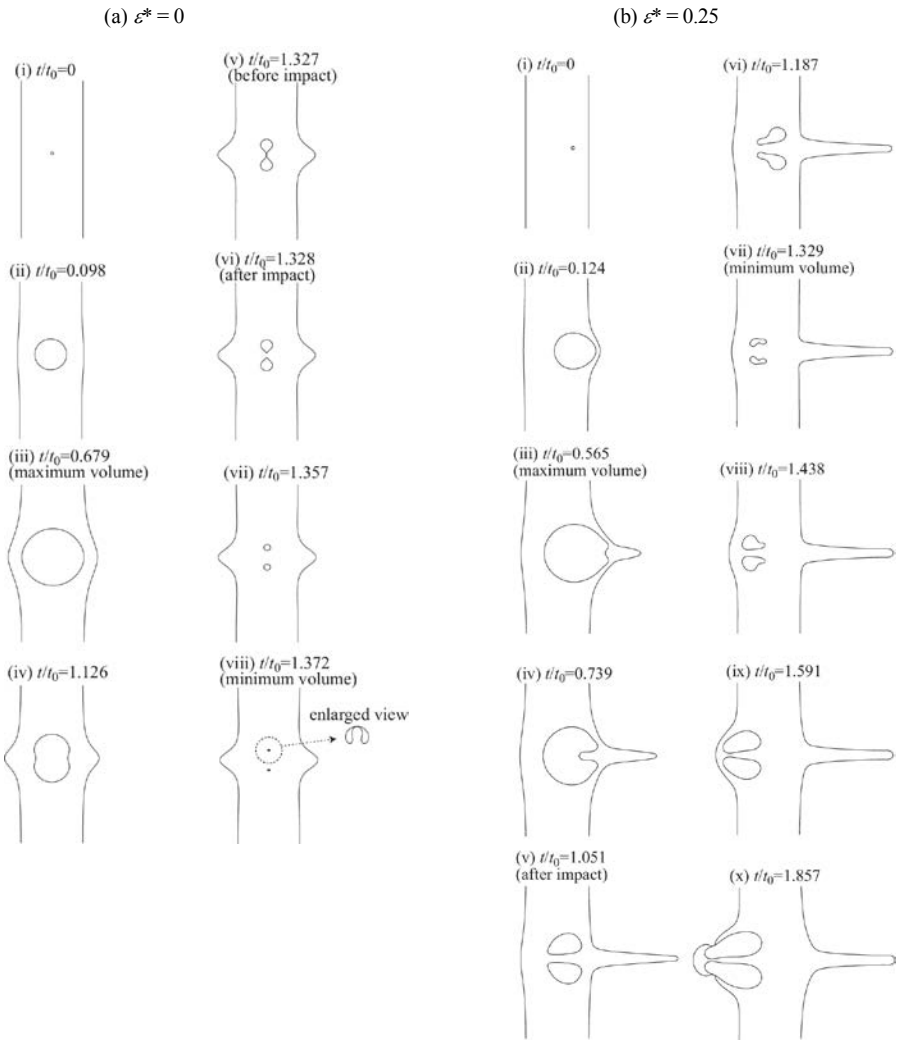

Figure 4 Successive bubble and free surface shapes simulated with the boundary element method ($R_{max}^* = 0.47$).

Since the liquid is assumed to be incompressible in the boundary element analysis, the physics of the shockwave cannot be treated. Therefore, we simulated the bubble collapse by solving Euler equations and a stiffened-gas equation of state [14] using the ghost fluid method [10-12] (GFM) with the level-set method [15, 16]. Initial conditions are given at the maximum expansion of a bubble: the initial shapes of the bubble and free surfaces are given from the corresponding numerical results of the boundary element analysis. The other initial conditions are as follows; $p_\infty = 10^8$ Pa, $\rho_0 = 1034$ kg/m^3, and $p_{g0}/p_\infty = 30$. Note that $t = 0$ in only this simulation indicates the time when the bubble takes the maximum volume. Figure 5 shows the successive Schlieren images in the symmetric arrangement ($\varepsilon^* = 0$) at $R_{max}^* = 0.46$ and 0.57. Under these conditions, the skirts of the water columns deform to be a concave shape during the bubble collapse. Then, shockwaves are emitted from the bubble due to the liquid-jet impact on the toroidal bubble surface and the rebounding motion. After that, the shockwaves propagate and reach the concaved free surface, which leads to the formation of ring-shaped inclined water columns shown in the last images in Fig. 5. This causes the crown-like shaped water column which is observed in the experiment after the first bubble collapse.

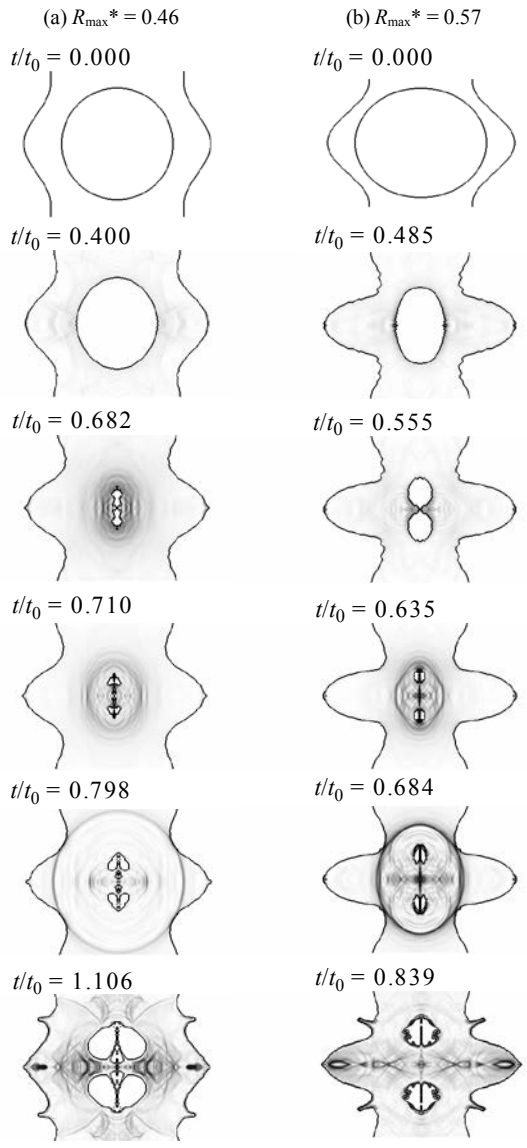

Figure 5 Successive Schlieren images with bubble and free surface shapes simulated with the ghost fluid method ($\varepsilon^* = 0$).

Conclusion

The growth and collapse of a bubble between two parallel free surfaces were investigated experimentally and numerically. In the experiment, the water column formations on the free surfaces are observed: one is the convex water column developing on the both free surfaces during the bubble growth, and the other is the crown-like shaped water column during the growth and collapse of a bubble collapse. The former water column tends to be formed only on the nearer free surface when the initial bubble position offsets from the center of a plane jet. The latter water column is formed by the liquid-jet and rebound shockwave from the collapsing bubble. When a bubble is generated at the center of the plane water jet, the bubble translation does not arise because of the symmetric arrangement of free surfaces to the bubble. The violent crown-like shaped water columns are developed on the closer free surfaces to the bubble. The bubble and free surface shapes in the simulation are qualitatively in good agreements with the corresponding experiments: the bubble is elongated toward the free surface at the maximum bubble volume, and a water column grows on each free surface during the first growth and collapse phases. It is shown that a shockwave is emitted from the bubble when the bubble becomes toroidal during the collapse. Also, another shockwave is emitted when the ring liquid-jet developed from the inner surface of the toroidal bubble impacts on the outer surface of the bubble. These shockwaves cause the generation of inclined crown-like shaped water columns on the free surfaces.

References

[1] Hassanein, A. (2000). *Liquid-metal targets for high-power applications: Pulsed heating and shock hydrodynamics*. Laser Part. Beams 18, 611–622.
[2] Chahine, G. L. (1977). *Interaction between an oscillating bubble and a free surface*. J. Fluid Eng. 99, 709–716.
[3] Blake, J. R. and Gibson, D. C. (1981). *Growth and collapse of a vapour cavity near a free surface*. J. Fluid Mech. 111, 123–140.
[4] Robinson, P. B. and Blake, J. R. (2001). *Interaction of cavitation bubbles with a free surface*. J. Appl. Phys. 89, 8225–8237.
[5] Tomita, Y. and Kodama, T. (2003). *Interaction of laser-induced cavitation bubbles with composite surfaces*. J. Appl. Phys. 94, 2809–2816.
[6] Zhang, S., Wang, S. P. and Zhang, A. M. (2016). *Experimental study on the interaction between bubble and free surface using a high-voltage spark generator*. Phys. Fluids. 28, 032109.
[7] Robert, E., Letty, J., Farhat, M., Monkewitz, P. A. and Avellan, F. (2007). *Cavitation bubble behavior inside a liquid jet*. Phys. Fluids. 19, 067106.
[8] Takahira, H., Murakami, K., Omori, H. Tanaka, S. and Kamiirisa, H. (2003). *Boundary element analysis of bubble collapse under a floating body*. Transactions of the Japan Society of Mechanical Engineers, B 69, 755–763 (in Japanese).
[9] Yasuda, A. and Takahira, H. (2003). *Numerical analysis of the dynamics of toroidal bubbles considering the heat transfer of internal gas*. JSME Int. J., Ser. B 46, 600–609.
[10] Fedkiw, R., Aslam, T., Merriman, B. and Osher, S. (1999). *A non-oscillatory Eulerian approach to interfaces in multimaterial flows (the ghost fluid method)*. J. Comput. Phys. 152(2), 457–492.
[11] Kobayashi, K., Jinbo, Y. and Takahira, H. (2011). *Application of multigrid ghost fluid method to the interaction of shock waves with bubbles in liquids*, Transactions of the Japan Society of Mechanical Engineers, B 77, 723–738 (in Japanese).
[12] Jinbo, Y., Ogasawara, T. and Takahira, H. (2015). *Influence of the nonequilibrium phase transition on the collapse of inertia nonspherical bubbles in a compressible liquid*. Exp. Therm. Fluid Sci. 60, 374–384.
[13] Best, J. P. (1993). *The formation of toroidal bubbles upon the collapse of transient cavities*. J. Fluid Mech. 251, 79–107.
[14] Saurel, R., Petitpas, F. and Abgrall, R. (2008). *Modelling phase transition in metastable liquids. Application to cavitation and flashing flows*. J. Fluid Mech. 607, 313–350.
[15] Sussman, M., Smereka, P. and Osher, S. (1994). *A level set approach for computing solutions to incompressible two-phase flow*. J. Comput. Phys. 114. 146–159.
[16] Enright, D., Fedkiw, R., Ferziger, J. and Mitchell, I. (2002). *A hybrid particle level set method for improved interface capturing*. J. Comput. Phys. 183. 83–116.